LETTERS

The cause of the fragile relationship between the Pacific El Niño and the Atlantic Niño

Ping Chang[1], Yue Fang[1], R. Saravanan[2], Link Ji[1] & Howard Seidel[1]

El Niño, the most prominent climate fluctuation at seasonal-to-interannual timescales, has long been known to have a remote impact on climate variability in the tropical Atlantic Ocean, but a robust influence is found only in the northern tropical Atlantic region[1]. Fluctuations in the equatorial Atlantic are dominated by the Atlantic Niño[2,3], a phenomenon analogous to El Niño, characterized by irregular episodes of anomalous warming during the boreal summer. The Atlantic Niño strongly affects seasonal climate prediction in African countries bordering the Gulf of Guinea[4,5]. The relationship between El Niño and the Atlantic Niño is ambiguous and inconsistent. Here we combine observational and modelling analysis to show that the fragile relationship is a result of destructive interference between atmospheric and oceanic processes in response to El Niño. The net effect of El Niño on the Atlantic Niño depends not only on the atmospheric response that propagates the El Niño signal to the tropical Atlantic, but also on a dynamic ocean–atmosphere interaction in the equatorial Atlantic that works against the atmospheric response. These results emphasize the importance of having an improved ocean-observing system in the tropical Atlantic, because our ability to predict the Atlantic Niño will depend not only on our knowledge of conditions in the tropical Pacific, but also on an accurate estimate of the state of the upper ocean in the equatorial Atlantic.

There is clear observational evidence that the anomalous warming in the eastern equatorial Pacific during an El Niño produces a warming signal in the troposphere as a result of increased atmospheric heating[6], which then propagates rapidly eastward in the form of an equatorial Kelvin wave and westward in the form of a Rossby wave, as predicted by simple theoretical models[7,8] (Fig. 1a). The tropospheric warming stabilizes the environment, causing reduced moist convection, which acts in conditionally unstable environments to redistribute energy from the boundary layer to the free troposphere. As a result, boundary layer energy, primarily in the form of latent heat that originates via evaporation from the ocean surface, will accumulate[9]. This then provides a 'back pressure' that reduces evaporation from the ocean surface to the boundary layer, leading to a warming of the ocean mixed layer. This so-called 'tropospheric temperature mechanism' is arguably an important driving mechanism for the tropical El Niño teleconnection[10,11]. In the deep tropical Atlantic, it works most effectively from late boreal winter to early spring when the sea surface temperature (SST) is warmest seasonally and the Intertropical Convergence Zone is closest to the Equator. The overall reduction of precipitation in the tropical Atlantic basin observed following El Niños is consistent with the weakening of moist convection[12]. Modelling studies[11,13] consistently show that in the absence of ocean dynamics a basinwide warming of the tropical Atlantic follows an El Niño.

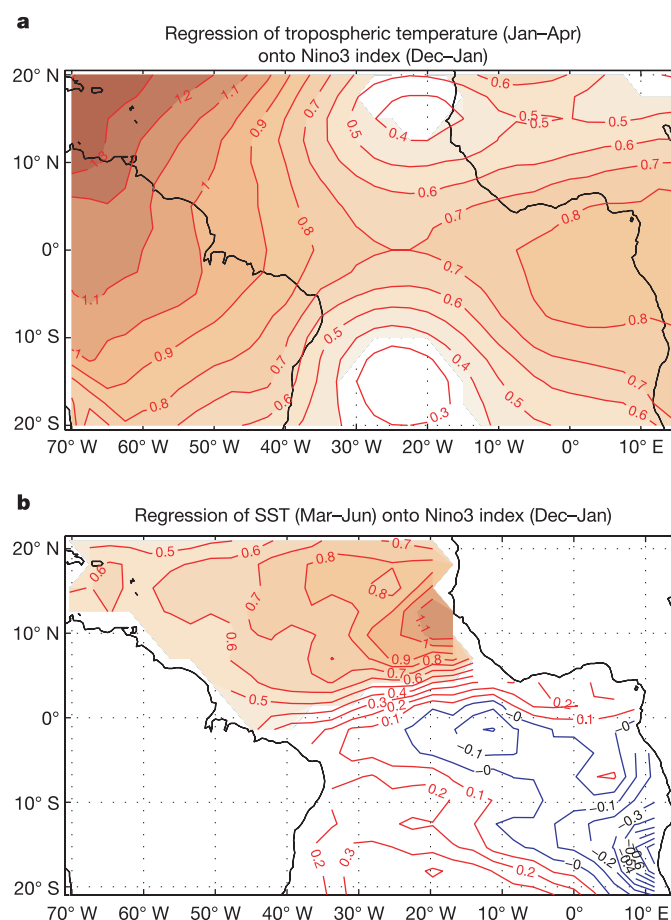However, the regressed SST response derived from observations

a

Regression of tropospheric temperature (Jan–Apr) onto Nino3 index (Dec–Jan)

b

Regression of SST (Mar–Jun) onto Nino3 index (Dec–Jan)

Figure 1 | Tropospheric and surface temperature response of the tropical Atlantic to El Niño revealed by a regression analysis. a, The regressed anomalous tropospheric temperature averaged between atmospheric pressure levels of 800 mbar and 200 mbar over January–April against the previous boreal winter, December–January, NINO3 SST (SST anomaly averaged over 150° W–90° W and 5° S–5° N). **b**, The similar regression of the observed March–June SST anomaly. The SST response is expected to lag the tropospheric temperature response because it is driven by surface heat fluxes. The mid-tropospheric temperatures were derived from the 43-year (1958–2000) reanalysis product, ERA40, of the European Centre for Medium-Range Weather Forecasts (ECMWF); http://www.ecmwf.int/research/era and the SST is from the Reynolds Optimum Interpolation SST[22] during the same period. The coloured shading shows areas that exceed a 99% significance level based on Student's *t*-test.

[1]Department of Oceanography, [2]Department of Atmospheric Sciences, Texas A&M University, College Station, Texas 77843, USA.
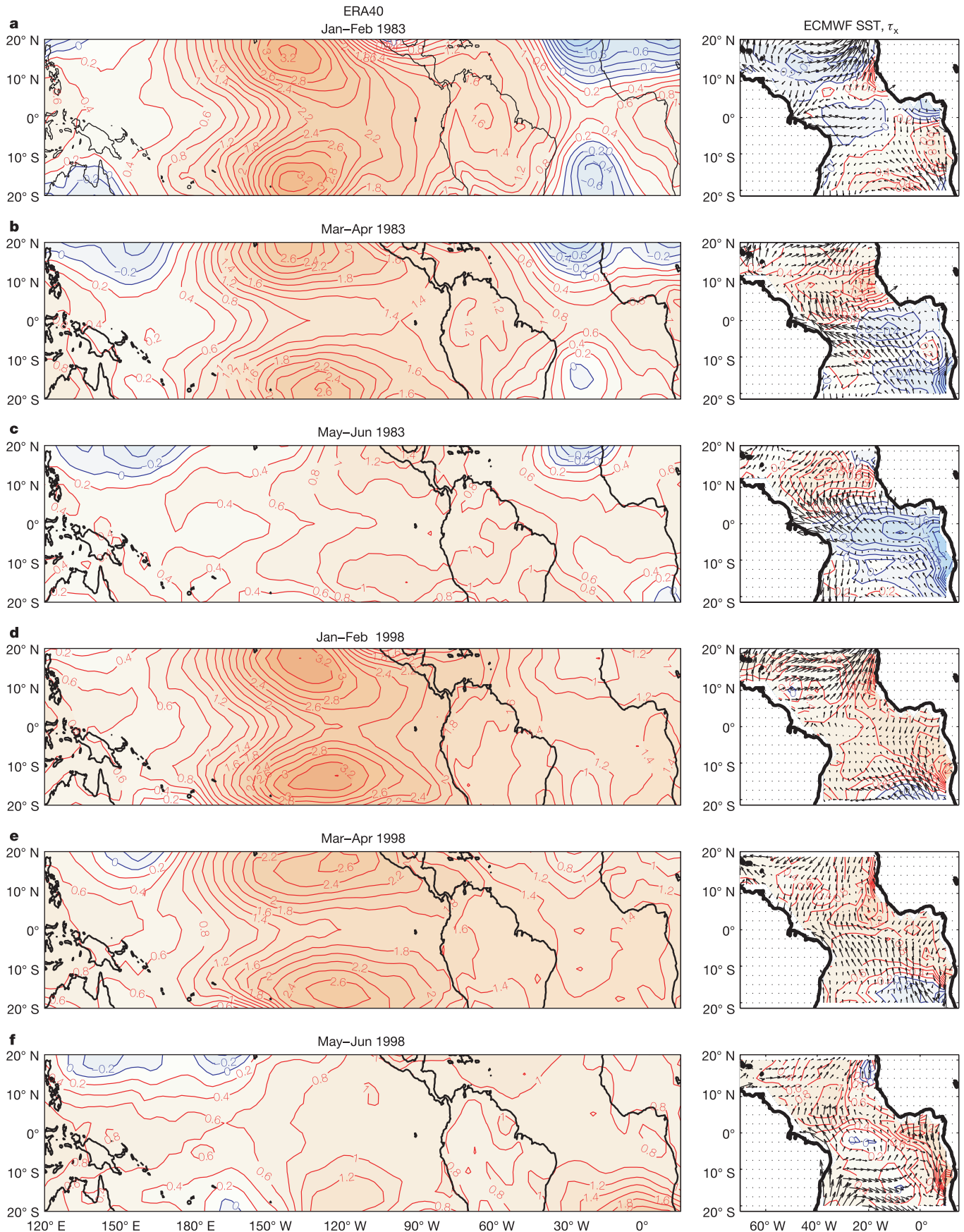
Figure 2 | **Atmospheric response to the 1982/83 and 1997/98 El Niños.** **a–c**, 1982/83; **d–f**, 1997/98. The left panels show the middle troposphere temperature anomaly averaged between atmospheric pressure levels of 800 mbar and 200 mbar, based on the ECMWF ERA40 reanalysis product. The right panels show the observed SST and surface wind stress (τ_x) anomaly from the same ECMWF and Reynolds SST products.

does not show a basinwide warming (Fig. 1b), as one would expect from the tropospheric temperature mechanism. The robust warming is found only in the north tropical Atlantic. This may be attributed partially to the fact that the tropospheric temperature mechanism works more efficiently in this region because of the warmer mean SST (ref. 11) and that El Niños can cause a weakening in the northeasterly trade wind, resulting in a further reduction in evaporative heat loss and thus enhancing the warming[12]. In the equatorial and south tropical Atlantic regions, however, the observed response is more perplexing: it tends to be opposite to that in the troposphere, albeit less statistically significant.

The lack of a robust and consistent response of the equatorial SST to El Niño can be made more evident by contrasting the tropospheric and surface response to the 1982/83 and 1997/98 El Niños, two of the strongest events in the instrumental record (Fig. 2). In spite of the well-defined tropospheric warming in both events, the surface responses are drastically different along the Equator and along the southern African coast: persistent surface warming was observed following the 1997/98 El Niño, consistent with the tropospheric temperature mechanism, while a cooling condition prevails in the wake of the 1982/83 El Niño. We wondered what physical factors cause the equatorial Atlantic to respond differently to these El Niños.

First, we considered the surface wind response in the western tropical Atlantic region. In the case of the 1982/83 El Niño, there is a well-defined easterly wind anomaly that persists from the late boreal winter to the early boreal summer in this region (Fig. 2). Such a wind

response is apparently much weaker during the 1997/98 El Niño. The relationship between the wind variability over the western tropical Atlantic and El Niño has previously been noted[14–16]. A correlation analysis between the observed NINO3 SST time series and the zonal wind stress anomaly reveals an extended area along the western equatorial Atlantic where the correlation coefficient is significantly negative for the months following the peak of El Niño (Fig. 3a). A closer examination reveals that all the El Niño events that did not produce a warming in the equatorial Atlantic were accompanied by anomalously strong easterly winds in this region, while those El Niños that did produce a warming did not have such strong wind anomalies (Fig. 3b).

A previous modelling study[16] suggested that El Niño may lead to cooling in the equatorial Atlantic. Dynamically, the equatorial cooling can be understood in terms of the Bjerknes feedback where, in this case, an easterly wind stress anomaly along the Equator acts to shoal the thermocline, enhancing the stratification and at the same time increasing the vertical entrainment rate on the eastern
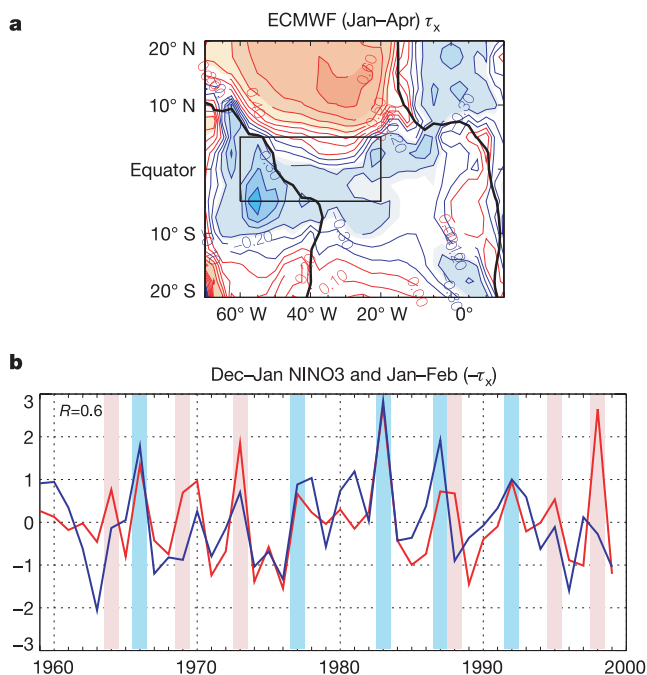

Figure 3 | Observed response of tropical Atlantic zonal wind stress to El Niño. a, Correlation between the December–January NINO3 index and the zonal wind stress anomaly from the ECMWF ERA-40 reanalysis product over the tropical Atlantic sector in the following January–April from 1958–2000. The blue contours indicate negative and the red contours positive correlation. The colour shade shows areas that exceed a 95% significance level based on Student's *t*-test. **b**, Normalized time series of the January–February wind stress index (with reversed sign) over the western equatorial region (60° W–20° W and 5° S–5° N) indicated by the rectangle in **a**, and the December–January NINO3 index. The correlation coefficient between the two indices is 0.6. The blue vertical bars indicate those El Niño events (1965/66, 1976/77, 1982/83, 1986/87 and the 1991/92 El Niño) that produced a strong easterly wind anomaly and the red indicate those (1963/64, 1968/69, 1972/73, 1987/88, 1994/95 and the 1997/98 El Niños) that did not.
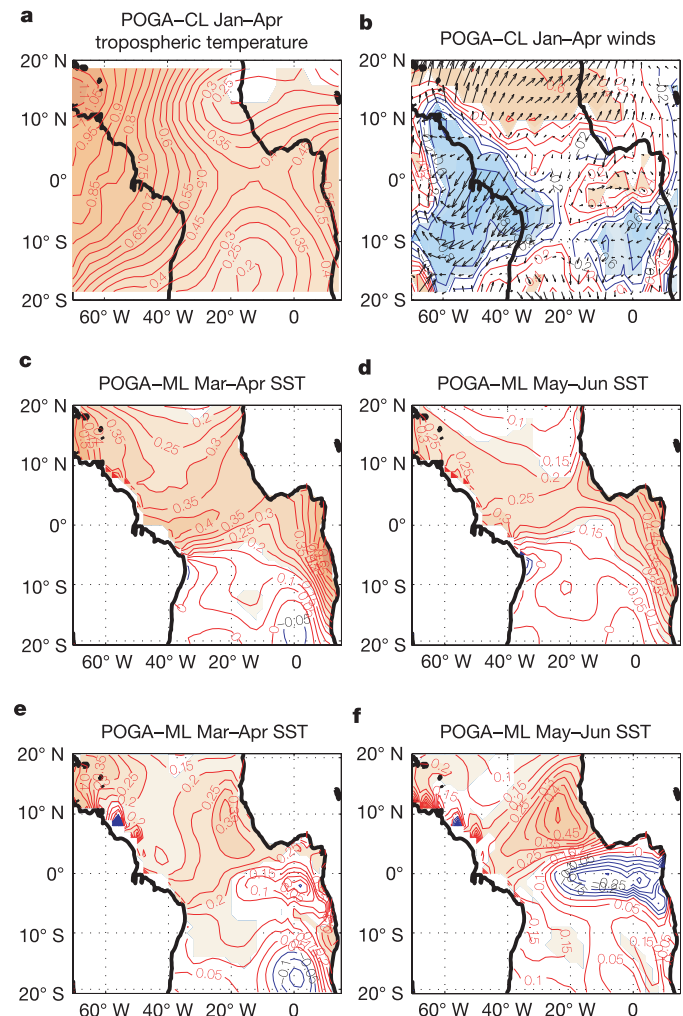

Figure 4 | The simulated tropical Atlantic response to El Niño in three ensembles of numerical experiments. a, b, Ensemble averaged regressions against the December–January NINO3 index from the POGA-CL runs for the January–April troposphere temperature (°C) averaged between atmospheric pressure levels of 800 mbar and 200 mbar (**a**) and surface winds (vectors; **b**), where the blue contours show the negative correlation of the zonal surface-wind with the NINO3 index and the red contours the positive. (**c–f**), Regressions of the ensemble averaged SST in March–April and May–June against the December–January NINO3 index from POGA-ML and POGA-RG runs. The colour shade shows areas that exceed a 99% significance level based on Student's *t*-test.

side of the basin, producing anomalous cooling at the surface. The atmosphere responds to this cooling by further strengthening the wind anomaly, forming a positive feedback between the ocean and atmosphere. We hypothesize that the cooling produced by the Bjerknes feedback competes with the tropospheric-temperature-induced warming. This competition is the main cause of the fragile relationship between the Pacific El Niño and the Atlantic Niño. Borrowing an analogy from wave theory, we refer to this process as 'destructive interference'.

It is difficult to test the destructive interference hypothesis solely on the basis of observational analysis, because observations always capture coupled variability and provide only a single realization of stochastic climate phenomena. We therefore turn to ensembles of coupled- and uncoupled-climate-model experiments (see Methods for model descriptions). The first ensemble of experiments—hereafter referred to as POGA-CL (see Methods)—is designed to examine the direct tropospheric and surface response of the atmosphere to El Niño. Figure 4a and b shows the atmospheric model ensemble mean response. It captures not only the observed structure of the tropospheric warming associated with El Niño (Fig. 1a), but also the surface wind response (Fig. 3a). In particular, the easterly wind anomaly in the western basin that is critically important to the Bjerknes feedback is well-simulated, indicating that the direct atmospheric response to El Niño is already sowing the seeds of the destructive interference.

We then conducted two additional ensembles of coupled-model experiments (hereafter referred to as POGA-ML and POGA-RG, respectively; see Methods). These experiments are specifically designed to test the destructive interference hypothesis by including both the thermodynamic and dynamic ocean–atmosphere interactions in the simulations. POGA-ML experiments, in which only the thermodynamic interaction is permitted, result in a surface warming taking place shortly after the peak of El Niño. The warming persists through the summer months along the Equator and along the southern African coast, as anticipated by the tropospheric temperature mechanism (Fig. 4c, d). Some of the warming along and to the north of the Equator can also be attributed to wind-induced latent heat flux changes[12]. In contrast, POGA-RG experiments, in which the dynamic interaction is also permitted, reveal a much weaker boreal spring equatorial warming and a cooling tendency during the early boreal summer (Fig. 4e, f). This cooling effect is attributed to the dynamic ocean response to the easterly surface wind anomaly associated with the warming in the troposphere. Further analyses indicate that the vertical advection of heat is primarily responsible for the cooling. A recent comprehensive coupled-climate study reports a similar finding[17]. Therefore, these modelling results support the destructive interference hypothesis as a plausible cause of the fragile relationship between the Pacific El Niño and the Atlantic Niño.

It is unclear what causes the winds in the western equatorial Atlantic to respond strongly to some El Niños, but not others, in spite of a significant overall correlation. One factor may be related to the pre-existing tropical Atlantic SST condition prior to an El Niño[18]. Model experiments where the annual cycle of Atlantic SST in the POGA-CL runs was replaced by the observed Atlantic SST show that a pre-existing warm SST anomaly may substantially weaken the wind response, resulting in a noticeable drop in the overall correlation between the western Atlantic wind index and NINO3. Another factor is related to stochasticity of the atmosphere. We noted that the correlation between the wind index derived from an individual ensemble member of the POGA-CL runs and the NINO3 can decrease from the ensemble mean correlation of over 0.8 to about 0.6 for individual members. Additionally, the wind response can depend on the atmospheric heating structure and duration, which can vary considerably from one El Niño to another.

The Atlantic Niño is not a simple passive response to the Pacific El Niño, but a complex one involving destructive interference between Pacific remote influence and Atlantic ocean–atmosphere feedback, making it a challenge for seasonal climate prediction. The SST anomaly in the equatorial Atlantic—a key climate variable for seasonal climate forecasts—depends on the relative dominance of the tropospheric-temperature-induced heating compared to the dynamic ocean–atmosphere feedback. Therefore, a successful forecast of SST not only requires that climate models simulate both processes accurately, but also requires an accurate estimate of the atmospheric state, both in terms of temperature and surface wind response to El Niño, and of the upper ocean state. The latter points to the necessity of an ocean observing system in the tropical Atlantic because an accurate estimate of the upper ocean state is crucial for determining the strength of the dynamic ocean–atmosphere feedback. In contrast, the ocean dynamics appear less critical in the north tropical Atlantic, for which even an atmospheric general circulation model coupled to a simple slab ocean is useful in forecasting seasonal SST anomalies[19].

METHODS

Models. The atmospheric model is the Community Climate Model version 3 (CCM3) developed at the National Center for Atmospheric Research with the standard configuration of T42 spectral truncation in the horizontal and 18 hybrid levels in the vertical. It incorporates a comprehensive suite of physical parameterizations including a non-local boundary layer parameterization and improved radiative and convection parameterizations[20]. The coupled model is comprised of the CCM3 as the atmospheric component and an extended 1.5-layer reduced-gravity ocean model that has been used extensively in the study of the Pacific El Niño[21] and also applied to the study of the Atlantic Niño[3]. The ocean model has a resolution of 2° in longitude by 1° in latitude and is coupled to the CCM3 in the tropical Atlantic sector (between 30° S and 30° N), outside which the atmospheric model is forced with observed SSTs.

POGA-CL experiments. The Pacific Ocean-Global Atmosphere (POGA)-Climatological (CL) ensemble simulation consists of nine runs where the CCM3 was forced with observed SSTs from 1950 to 1995 in the Pacific and with the annual cycle of SST in the Atlantic. Each ensemble member differs only slightly in its atmospheric initial condition.

POGA-ML experiments. The POGA-Mix Layer (ML) ensemble simulation consists of 12 runs where, in the Pacific sector, the coupled model was forced with observed SSTs from 1980 to 2000. In the tropical Atlantic sector where the model is coupled, the ocean component had all the dynamic processes (except diffusion) disabled, so that the ocean model essentially degenerates to a slab ocean where SST changes are completely determined by atmospheric surface heat fluxes. As in POGA-CL, each ensemble member differs only slightly in its atmospheric initial condition.

POGA-RG experiments. The POGA-Reduced Gravity (RG) ensemble simulation is identical in set-up to POGA-ML, except that all the dynamic processes of the reduced-gravity ocean model are retained.

1. Enfield, D. B. & Mayer, D. A. Tropical Atlantic SST variability and its relation to El Niño–Southern Oscillation. *J. Geophys. Res.* **102**, 929–945 (1997).
2. Merle, J. Variabilité thermique annuelle et interannuelle de l'océan Atlantique équatorial Est. L'hypothése d'un "El Niño" Atlantique. *Oceanol. Acta* **3**, 209–220 (1980).
3. Zebiak, S. E. Air–sea interaction in the equatorial Atlantic region. *J. Clim.* **6**, 1567–1586 (1993).
4. Goddard, L. & Mason, S. J. Sensitivity of seasonal climate forecasts to persisted SST anomalies. *Clim. Dyn.* **19**, 619–632 (2002).
5. Giannini, A., Saravanan, R. & Chang, P. Oceanic forcing of Sahel rainfall on interannual to interdecadal time scales. *Science* **302**, 1027–1030 (2003).
6. Yulaeva, E. & Wallace, J. M. Sensitivity of seasonal climate forecasts to persisted SST anomalies. *J. Clim.* **7**, 1719–1736 (1994).
7. Gill, A. E. Some simple solutions for heat-induced tropical circulation. *Q. J. R. Meteorol. Soc.* **106**, 447–462 (1980).
8. Saravanan, R. & Chang, P. Interaction between tropical Atlantic variability and El Niño–Southern Oscillation. *J. Clim.* **13**, 2177–2194 (2000).
9. Brown, R. G. & Bretherton, C. S. A test of the strict quasi-equilibrium theory on long time and space scales. *J. Atmos. Sci.* **54**, 624–638 (1997).
10. Chiang, J. C. H. & Sobel, A. H. Tropical tropospheric temperature variations caused by ENSO and their influence on the remote tropical climate. *J. Clim.* **15**, 2616–2631 (2002).
11. Chiang, J. C. H. & Lintner, B. R. Mechanisms of remote tropical surface warming during El Niño. *J. Clim.* **18**, 4130–4149 (2005).

12. Giannini, A., Chiang, J. C. H., Cane, M. A., Kushnir, Y. & Seager, R. The ENSO teleconnection to the tropical Atlantic Ocean: contributions of the remote and local SSTs to rainfall variability in the tropical Americas. *J. Clim.* **15**, 4530–4544 (2001).
13. Alexander, M. & Scott, J. The influence of ENSO on air–sea interaction in the Atlantic. *Geophys. Res. Lett.* **29**, doi:10.1029/2001GL014347 (2002).
14. Delecluse, P., Servain, J., Levy, C., Arpe, K. & Bengtsson, L. On the connection between the 1984 Atlantic warm event and the 1982–1983 ENSO. *Tellus A* **46**, 448–464 (1994).
15. Carton, J. A. & Huang, B. Warm events in the tropical Atlantic. *J. Phys. Oceanogr.* **24**, 888–903 (1994).
16. Latif, M. & Barnett, T. P. Interactions of the tropical oceans. *J. Clim.* **8**, 952–964 (1995).
17. Huang, B. Remotely forced variability in the tropical Atlantic Ocean. *Clim. Dyn.* **23**, 133–152 (2004).
18. Giannini, A., Saravanan, R. & Chang, P. The preconditioning of tropical Atlantic variability in the development of the ENSO teleconnection: implications for the prediction of Nordeste rainfall. *Clim. Dyn.* **22**, 839–855 (2004).
19. Chang, P., Saravanan, R. & Ji, L. Tropical Atlantic seasonal predictability: the roles of El Niño remote influence and thermodynamic air–sea feedback. *Geophys. Res. Lett.* **30**, 1501–1504 (2003).
20. Kiehl, J. T., Hack, J. J., Bonan, G. B., Boville, B. A., Williamson, D. L. & Rasch, P. J. The National Center for Atmospheric Research Community Climate Model: CCM3. *J. Clim.* **11**, 1131–1149 (1998).
21. Zebiak, S. E. & Cane, M. A. A model El Niño–Southern Oscillation. *Mon. Weath. Rev.* **115**, 2262–2278 (1987).
22. Reynolds, R. W. & Smith, T. M. Improved global sea surface temperature analysis using optimum interpolation. *J. Clim.* **7**, 929–948 (1994).